Plasma microstructure in the solar wind

B.T. TSURUTANI

Jet Propulsion Laboratory - Pasadena, California

G.S. LAKHINA

Indian Institute of Geomagnetism - Colaba, Mumbai/Bombay, India

Summary. — We review some of the new NASA/ESA Ulysses solar wind microscale results. Rotational discontinuities are shown to be the steepened edges of nonlinear Alfvén waves. These waves are arc-polarized and believed to be spherical (non-planar) in nature. Magnetic Decreases (MDs) are small spatial scale (2-3 proton gyroradii), field magnitude decreases. The field decreases are as large as 80% of the ambient field strength and are bounded by discontinuities. The properties of MDs are discussed. A theory of cross-magnetic field diffusion due to particle interactions with MDs will be briefly reviewed and summarized. This cross-field diffusion model can easily be generalized to astrophysical plasma cases where there are significant magnetic field gradients present.

PACS 96.50 – Interplanetary space.

1. – Introduction

The NASA/ESA Ulysses field and plasma mission is the first to go substantially out of the solar ecliptic plane. The orbit is shown in Fig. 1. The spacecraft was launched in October 1990. Ulysses first went to Jupiter to change its orbital plane by gravitational assist. The spacecraft obtained a highly elliptical orbit that passes within 10° of the

TABLE I. – *Mass flux and jump conditions across discontinuities.*

Type of Discontinuity	ρV_n	$[\vec{H}]$	
Rotational discontinuity	$\neq 0$	$[\vec{H}_t] = 0$	$H_n \neq 0$
Tangential discontinuity	0	$[\vec{H}_t] \neq 0$	$H_n = 0$
Shock	$\neq 0$	$[\vec{H}_t] \neq 0$ $[H_t] \neq 0$	$H_n \neq 0$
Contact discontinuity	0	$[\vec{H}_t] = 0$	$H_n \neq 0$

solar north and south poles (at $\sim \pm 80°$). We review the microscale plasma structures discovered near the solar polar regions and the implications that the structures have for the evolution of the solar wind and the scattering of energetic solar particles and low energy cosmic rays.

The types of magnetohydrodynamic (MHD) discontinuities that can theoretically exist have previously been discussed by Landau and Lifschitz [1]. The discontinuity properties are summarized in Table I. The discontinuities are listed in order of their frequency of occurrence in the solar wind: rotational discontinuities (the most frequently occurring; hereafter called RDs), tangential discontinuities (TDs), shocks, and contact discontinuities (CDs).

RDs and TDs are the most common structures found in the solar wind, and thus most of this paper will be devoted to these two phenomena. A variety of shocks (fast forward, fast reverse, slow forward and slow reverse) have been reviewed in Tsurutani and Stone [2], Stone and Tsurutani [3], and Ho *et al.* [4], respectively, and will not be covered here. The possibility that RDs are a form of (intermediate) shock has been noted and will be discussed. Finally, contact discontinuities have not been detected in interplanetary space and are not particularly interesting from a physical sense. These will not be discussed.

MHD RDs have no mass flux change across their structures, *e.g.*, ρV_n is constant (ρ is the density and V_n is the velocity component in the discontinuity normal direction). The normal component of the magnetic field (H_n) is nonzero and constant, while the direction of the tangential component can change. For TDs, there is no mass flow across the surface ($\rho V_n = 0$), and there is no field component normal to its surface. The tangential field direction and magnitude can change, however.

In Table I, we have described the discontinuity properties primarily in terms of the magnetic fields. In space plasmas, the measurement of magnetic fields is standardly quite rapid, and therefore useful for discontinuity diagnostic purposes. Plasma measurements are generally substantially slower. Although this lower rate information is useful (solar wind bulk parameters such as speed, temperature, composition, etc.) to obtain, the low cadence is typically not helpful for discontinuity analyses.

The above comments are applicable for idealized MHD cases. We use this as a starting

point to provide a general picture. However, it should be noted that the plasma is not always isotropic, and several such cases will be illustrated later.

Figure 2 illustrates schematics of what a RD and a TD would look like in 3-dimensions. A RD can be thought of as a sharply kinked Alfvén wave. Later we will show how accurate and applicable such a description is. A TD is an imaginary surface separating two dissimilar plasmas. Ordinarily there are no plasma or fields crossing its surface. However, when such structures do not have infinite extents, energetic particles can and will diffuse across their surfaces. This topic will be discussed later.

Directional discontinuities (DDs) are selected by a computer program applied to 1 min. average magnetic field data. In brief, one set of criteria [5] that has been used to identify DDs is

$$(\frac{|\Delta\vec{B}|}{B_0}) \geq 0.5$$

$$|\Delta\vec{B}| = 2\sqrt{\frac{1}{N}\sum_{i=1}^{N}(B_{i+1} - B_i)^2}$$

where $\Delta\vec{B}$ is the change in the field across the DD, B_0 is the ambient magnetic field, and B_i the individual 1 min. vectors. The criteria requires that the field change be significant in comparison to the ambient field and large relative to the statistical fluctuations in the field. Further details of this selection criteria can be found in Tsurutani and Smith [5]. This was the first computer-applied criteria developed to identify discontinuities. A second method has been identified by Lepping and Behannon [6]. These two methods will be identified as TS and LB, respectively. The principles behind the TS and LB criteria are quite similar and there is little to distinguish between them. The TS criteria are a little less stringent than the LB criteria, so (percentage-wise) the TS method detects more events.

Rates of occurrence of interplanetary discontinuities (ROIDs) in the ecliptic plane have been noted to be highly variable [7]. Values as high as 100 events/day and as low as zero per/day have been reported. After Ulysses went past Jupiter and started to go to strongly southern latitudes, a surprising observation was noted: there was a 25-day periodicity in occurrence rate and this periodicity was in-phase with a 25-day periodicity in the solar wind speed. These periodicities and the correlation between the two parameters can be noted in Fig. 3.

The panels of Fig. 3 are, from top to bottom: the plasma density, proton temperature, solar wind speed, magnetic field magnitude, discontinuity occurrence rates (both TS and LB) and spacecraft location (distance from the Sun and heliographic latitude). The solar wind speed varies from a low of $\sim$ 450 km s^{-1} to a high close to $\sim$ 750 – 800 km s^{-1}. The high-speed streams come from a coronal hole region of the Sun [8] [9], and thus they "corotate" with the Sun. "Coronal holes" are so named because they appear as dark "holes" in the corona when viewed in soft x-rays. The rate of DDs has a value of $\sim 10 - 20$ day^{-1} in the minimum velocity regions and $\sim 70 - 90$ day^{-1} at/near the velocity maxima. Near the right-hand side of the plot, Ulysses reached midlatitudes where it became permanently embedded in the high-speed stream. The velocity remained

at $\sim$ 750 to 800 km s^{-1}. Correspondingly, the DD occurrence rates went to a maximum of $\sim 70 - 90$ day^{-1}. Clearly the DD occurrence rate was higher within the high-speed streams.

The possibility that the periodic increases in DD detected occurrence rate is due to the (periodically) higher solar wind convection speeds was examined in Tsurutani *et al.* [7]. The distribution of discontinuity thicknesses was empirically determined. From the distribution and assuming a convection speed of 750 km s^{-1}, the rate of DD detection using the TS criteria was calculated. It was found that the higher speeds could lead to a maximum factor of $\sim$ 100% increase in DD detection rates, but not a factor of $5 - 10$ times higher, as observed (Fig. 3). Another explanation had to be sought.

Figure 4 shows the magnetic field and plasma velocity components in solar heliospheric (SH) coordinates. In this coordinate system, $\hat{X}$ points radially outward from the Sun, $\hat{Y} = \hat{\Omega} \times \hat{X}/|\hat{\Omega} \times \hat{X}|$ where $\hat{\Omega}$ is the rotation axis of the Sun, and $\hat{Z}$ forms a right-hand system. It should be noted that the entire interval is composed of large amplitude nonlinear fluctuations. $\vec{B}$ and $\vec{V}$ are correlated at zero lag (not shown), indicating that these fluctuations are Alfvénic and the waves are propagating outward from the Sun.

The Alfvén wave spectra have been examined in a number of different positions within the high-speed streams, and they seem to have the same properties, to first order [7]. The DD occurrence rates over the north and south polar regions were determined. Even though the passes occurred one year apart, the rates were basically the same [10].

Figure 5 shows one case of the relationship between slowly rotating Alfvén waves and DDs. The field is displayed in the minimum variance system where B_1 is the field in the direction of maximum variance, B_2 the component in the intermediate variance direction, and B_3 is the component in the direction of minimum variance [11] [12]. From point 1 to point 2, the B_1 component of the field increases slowly.

The hodogram at the bottom of the figure shows an arc-like rotation of the field for this interval. The discontinuity between points 2 and 3 leads to a rapid rotation back to the original field orientation. This rotation occurs as an arc (bottom inset) and lies in the same plane as the rotation from point 1 to 2 (not shown). There is a modest field magnitude change ($< 10\%$) at the discontinuity.

The DD is found to be rotational in nature. From the hodogram (and other similar cases), it has been concluded that the RDs and the slow field rotations are parts of the same structures. These are arc-polarized Alfvén waves that have phase steepened fronts (such structures cannot be described by MHD, but MHD gives very useful idealistic constructs).

Because the magnetic field magnitude remains constant (to first order) throughout the wave, the tip of the field vector must reside on the surface of a sphere. A schematic of different types of "polarizations" for spherical waves is given in Fig. 6. One can note that arc-polarization is one possibility. It is the nonlinear extension of linear polarized waves.

The properties of phase-steepened Alfvén waves have been explored theoretically. Medvedev *et al.* [13] and Buti *et al.* [14] have demonstrated that such waves would be expected to be dissipative and have many properties of intermediate shocks. Such dissi-

pative energy would heat the solar wind plasma and could have a substantial influence on the solar wind's evolution, depending, of course, on the rate of dissipation.

The possibility of dissipation of the phase-steepened Alfvén waves was explored. This is shown in Fig. 7. The normalized jumps in proton temperature, density and magnetic field magnitude across the RDs are shown in the three panels. Since the Alfvén waves are propagating/convecting more or less radially outward, a consistent upstream/downstream based analysis was easily conducted. For the panels, the convention used to calculate a normalized "change" is the antisolar side value less the solar side value divided by the antisolar side value. The normalized change has been plotted in a histogram format.

The proton temperature, proton density and magnetic field magnitude show no systematic jumps across the RDs. There are changes at the $5 - 10\%$ level, but these seem to be statistical fluctuations, rather than any systematic increases or decreases. If there are systematic plasma and field changes across RDs due to wave dissipation, they are slow relative to the time scales used in the analyses.

2. – Magnetic Decreases

Although the existence of tangential discontinuities has been well established for decades [15] [16] [17] , it was a surprise to find that TDs existed at high heliographic latitudes and at approximately the same rates $(5 - 12\%)$ as in the ecliptic plane [18]. Many researchers were surprised because it had been assumed that TDs were primarily associated with heliospheric current sheets (HCSs), and/or their filamentation [19] [20], and also plasma layers within coronal mass ejection (CME) loops, magnetic clouds, etc. [21]. Burlaga *et al.* [22] have suggested that pairs of similarly oriented TDs could bound magnetic "flat" noodles of field in the solar wind. As expected, the HCSs and CMEs were not detected at high latitudes and TDs associated with their internal structures were absent near the solar poles.

A new phenomenon was discovered at high latitudes called magnetic decreases (MDs). These are significant decreases in the field magnitude. MDs are typically bounded by discontinuities. Figure 8 shows three examples of MDs, plotted in SH coordinates. We have selected different "types" of MDs to illustrate how different the internal field changes can be. The important and consistent feature of MDs is that the discontinuities typically occur in pairs and bound decreases in the magnetic field magnitude.

The MD in the top panel is one where there is simply a decrease in the field magnitude. It is bounded by two TDs. The field before and after the MD have approximately the same magnitude and orientation.

The second panel illustrates a case where there are both significant field magnitude changes and field orientation changes across the MD. The field decreases from 1.2 nT to 0.8 nT and the B_R and B_N components reverse sign across the MD. The MD is bounded by two TDs.

The final example shows a MD again bounded by two TDs. The field magnitude does not change from one side to the other, but the orientation does change substantially. The

B_T component changes gradually over the whole MD while B_N changes abruptly at the second TD.

The minimum scale sizes of MDs were sought for Day 257, 1994, a region over the south pole. The examples are shown in the highest time resolution available in Fig. 9. The coordinate system is the same as in Fig. 8. The thicknesses are $\sim$ 20 s to 30 s. Assuming a proton speed of $\sim$ 750 km s^{-1}, the same as for the solar wind, this thickness corresponds to $\sim 2-3$ proton gyroradii.

Ho *et al.* [18] have suggested that MDs may be generated by the mirror instability operating closer to the Sun with those structures then convected to Ulysses distances. The instability criteria for mirror mode growth is:

$$\beta_\perp/\beta_\parallel > 1 + \frac{1}{\beta_\perp}$$

This condition is not satisfied in the regions adjacent to the MDs, thus the speculation of generation closer to the Sun.

129 discontinuities bounding MDs have been examined using the minimum variance technique. The results are given in Fig. 10. B_L is the larger field magnitude on either side of the MD. This format of plotting discontinuities in "phase space" has been adapted from Smith [17]. Discontinuities with large field magnitude changes ($\Delta|B|/B_L > 0.2$) and small normals ($B_n/B_L < 0.2$) are TDs. Those with large normals have properties of RDs. One can note that all discontinuities bounding MDs are not clear TDs. There are many cases where large fields in the normal direction are present. The normalized B_n/B_L values are clearly a continuum.

The minimum field within the MD normalized to the field outside is a continuum. This is shown in Fig. 11. The largest number of events occurs for cases when the field magnitude changes only slightly.

The MD thickness distribution is given in Fig. 12. The normal to the surface has been taken into account in this analysis. This figure corresponds to MDs when $\Delta|B|/B_L \geq 0.2$. Other (larger) thresholds for field decreases were examined, with similar results obtained.

At this time, it is unclear what mechanism is responsible for the formation of MDs, where they are formed and what evolution is taking place. It appears that events that have large field normals at their boundaries may have magnetic field reconnection in progress. It is also unclear whether some of these events are due to the mirror mode instability or not. Such a mechanism for formation does not explain the presence of discontinuities at their boundaries.

3. – Cross-Field Diffusion

Energetic particles that interact with the MDs can be "scattered" across magnetic fields. Each interaction leads to a finite and well defined cross-field displacement. Interactions with many MDs leads to diffusion. The single interaction and the basis of cross-field motion is given in Fig. 13. Our first-cut model assumes that the MD is a simple decrease in field magnitude with no change in direction. The field is assumed to

be constant inside and outside the MD. The field outside the MD is B_0 and within the MD, B_{MD}. The MD is assumed to have a circular cross-section, of radius a.

Figure 13 illustrates an ion gyrating in a magnetic field that is directed out of the paper. The origin (guiding center) is originally at point O. The ion impacts the MD at point P_1. Because of the decrease of the field inside the MD, the particle gyroradius is increased to $r = r_0\ (B_0/B_{MD})$, where r_0 is the original gyroradius $(O - P_1)$. The new gyro-center is at point O'. The particle then gyrates across to point P_2 where the gyroradius is reduced to its original value r_0. The center of gyromotion will be point O''. Thus from the particle interaction with the MD, the particle guiding center has moved from point O to point O''.

Figure 14 gives the geometry for a proton-MD interaction. The "impact parameter", d, is defined as the distance between the ion gyrocenter and the MD center.

The diffusion coefficient is defined as:

$$D_\perp = \frac{<\lambda^2>}{\Delta t}$$

where λ is the cross-field distance, *i.e.*, $O - O''$ as in Fig. 13, and Δt is the time between interactions. After working through the relevant geometrical considerations (discussed in Tsurutani *et al.* [23]), this can be expressed as

$$D_\perp = \frac{(M-1)^2}{2aM^2\Delta t} \times$$
$$\left[\frac{2a}{3}([2M+3]\,a^2 + 3M^2r^2) + \frac{(a^2-M^2r^2)^2}{[M(M-1)(Mr^2-a^2)]^{\frac{1}{2}}} \tanh^{-1}\left(\frac{2a[M(M-1)(Mr^2-a^2)]^{\frac{1}{2}}}{a^2-M(2-M)r^2}\right)\right]$$

where $M = B_0/B_{MD}$. Δt is equal to $L/V_\parallel$ where L is the distance between MDs and $V_\parallel$ is the parallel velocity along the magnetic field.

Clearly the above analyses can be generalized, so the assumptions can be removed. The MD need not be circular in cross section, the fields need not be oriented in the same direction within the MD and the fields need not be uniform within the MD and outside the MD. One point to make is that by relaxing the constraints, it can be seen that general magnetic field gradients present in an astrophysical plasma will lead to cross-field diffusion of energetic charged particles.

* * *

Portions of this work were performed at the Jet Propulsion Laboratory, California Institute of Technology, under contract with the National Aeronautics and Space Administration, Washington D.C.

REFERENCES

[1] LANDAU L.D. and LIFSHITZ E.M., *Electrodynamics of Continuous Media*, (Pergamon, New York) 1960.

[2] TSURUTANI B.T. and STONE R.G., *Collisionless Shocks in the Heliosphere, Reviews of Current Research*, (Am. Geophys. Union, Washington D.C.) 1985.

[3] STONE R.G. and TSURUTANI B.T., *Collisionless Shocks in the Heliosphere, A Tutorial Volume*, (Am. Geophys. Union, Washington D.C.) 1985.

[4] HO C.M., TSURUTANI B.T., LIN N., LANZEROTTI L.J., SMITH E.J., GOLDSTEIN B.E., BUTI B., LAKHINA G.S. and ZHOU X.-Y., *A pair of forward and reverse slow-mode shocks detected by Ulysses at ~ 5 AU, Geophys. Res. Lett.*, **25** (1998) 2613

[5] TSURUTANI B.T. and SMITH E.J., *Interplanetary discontinuities: Temporal variations and the radial gradient from 1 to 8.5 AU, J. Geophys. Res.*, **84** (1979) 2773

[6] LEPPING R.P. and BEHANNON K.W., *Magnetic field directional discontinuities: Characteristics between 0.46 and 1.0 AU, J. Geophys. Res.*, **91** (1986) 8725

[7] TSURUTANI B.T., HO C.M., ARBALLO J.K., SMITH E.J., GOLDSTEIN B.E., NEUGEBAUER M., BALOGH A. and FELDMAN W.C., *Interplanetary discontinuities and Alfvén waves at high heliographic latitudes: Ulysses, J. Geophys. Res.*, **101** (1996) 11027

[8] PHILLIPS J.L., BALOGH A., BAME S.J., GOLDSTEIN B.E., GOSLING J.T., HOEKSEMA J.T., MCCOMAS D.J., NEUGEBAUER M., SHEELEY N.R. JR. and WANG Y.M., *Ulysses at 50° south: Constant immersion in the high speed solar wind, Geophys. Res. Lett.*, **21** (1994) 1105

[9] MCCOMAS D.J., GOSLING J.T., BAME S.J., SMITH E.J. and CANE H.V., *A test of magnetic field draping induced B_Z perturbations ahead of fast coronal mass ejecta, J. Geophys. Res.*, **94** (1989) 1465

[10] TSURUTANI B.T., HO C.M., SAKURAI R., GOLDSTEIN B.E., BALOGH A. and PHILLIPS J.L., *Symmetry in discontinuity properties at the north and south heliospheric poles: Ulysses, Astron. Astrophys.*, **316** (1996) 342

[11] SONNERUP B.U.Ö. and CAHILL L.J. JR., *Magnetopause structure and attitude from Explorer 12 observations, J. Geophys. Res.*, **72** (1967) 171

[12] SMITH E.J. and TSURUTANI B.T., *Magnetosheath lion roars, J. Geophys. Res.*, **81** (1976) 2261

[13] MEDVEDEV M.V., DIAMOND P.H., SHEVCHENKO V.I. and GALINSKY V.L., *Dissipative dynamics of collisionless nonlinear Alfvén wave trains, Phys. Rev. Lett.*, **78** (1997) 4934

[14] BUTI B., GALINSKI V.L., SHEVCHENKO V.I., LAKHINA G.S., TSURUTANI B.T., GOLDSTEIN B.E., DIAMOND P. and MEDVEDEV M.V., *Evolution of nonlinear Alfvén waves in streaming inhomogeneous plasmas, Astrophys. J.*, **524** (1999)

[15] COLBURN D.S. and SONETT C.P., *Discontinuities in the solar wind, Space Sci. Rev.*, **5** (1966) 439

[16] BURLAGA L.F., *Nature and origin of directional discontinuities in the solar wind, J. Geophys. Res.*, **76** (1971) 4360

[17] SMITH E.J., *Identification of interplanetary tangential and rotational discontinuities, J. Geophys. Res.*, **78** (1973) 2054

[18] HO C.M., TSURUTANI B.T., GOLDSTEIN B.E., PHILLIPS J.L. and BALOGH A., *Tangential discontinuities at high heliographic latitudes (~ −80°), Geophys. Res. Lett.*, **22** (1995) 3409

[19] SMITH E.J., NEUGEBAUER M., BALOGH A., BAME S.J., ERDOS G., FORSYTH R.J., GOLDSTEIN B.E., PHILLIPS J.L. and TSURUTANI B.T., *Disappearance of the heliospheric sector structure at Ulysses, Geophys. Res. Lett.*, **20** (1993) 2327

[20] CROOKER N.U., BURTON M.E., PHILLIPS J.L., SMITH E.J. and BALOGH A., *Heliospheric plasma sheets as small-scale transients, J. Geophys. Res.*, **101** (1996) 2467

[21] TSURUTANI B.T., ARBALLO J.K., LAKHINA G.S., HO C.M., AJELLO J., PICKETT J.S., GURNETT D.A., LEPPING R.P., PETERSON W.K., ROSTOKER G., KAMIDE Y. and KOKUBUN S., *The January 10, 1997 auroral hot spot, horseshoe aurora and first substorm: A CME loop?, Geophys. Res. Lett.*, **25** (1998) 3047

[22] BURLAGA L.F., *Directional discontinuities in the interplanetary magnetic field, Sol. Phys.*, **7** (1969) 54

[23] TSURUTANI B.T., LAKHINA G.S., GALVAN C., SAKURAI R., GOLDSTEIN B.E. and NEUGEBAUER M., *Energetic particle cross-field diffusion: Interaction with magnetic decreases*, *Nonlin. Proc. Geophys.*, **in press** (1999)

APPENDIX A.

Figure captions

Fig. 1. - The Ulysses orbit about the Sun.
Fig. 2. - Schematics of an idealized rotational discontinuity (left panel) and an idealized tangential discontinuity (right panel).
Fig. 3. - Post-Jupiter plasma, magnetic field, and discontinuity rates as Ulysses goes to southerly latitudes.
Fig. 4. - Alfvénic fluctuations detected at the south heliospheric pole by Ulysses.
Fig. 5. - Relationship between an Alfvén wave and a discontinuity. The waves are spherical waves with arc polarization.
Fig. 6. - Different types of polarizations for spherical waves. The bottom panel illustrates "arc" polarization.
Fig. 7. - Normalized temperature, density, and magnetic field magnitude jumps across arc polarized discontinuities.
Fig. 8. - Three examples of magnetic decreases (MDs).
Fig. 9. - Two examples of very small MDs at the solar south pole. The scale size is 2-3 r_p.
Fig. 10. - Distribution of normals of the discontinuities bounding MDs.
Fig. 11. - Distribution of the magnetic field magnitude changes within MDs.
Fig. 12. - Distribution of MD spatial thicknesses.
Fig. 13. - Schematic of motion of a particle guiding center across magnetic fields.
Fig. 14. - A model of an ion-MD interaction.

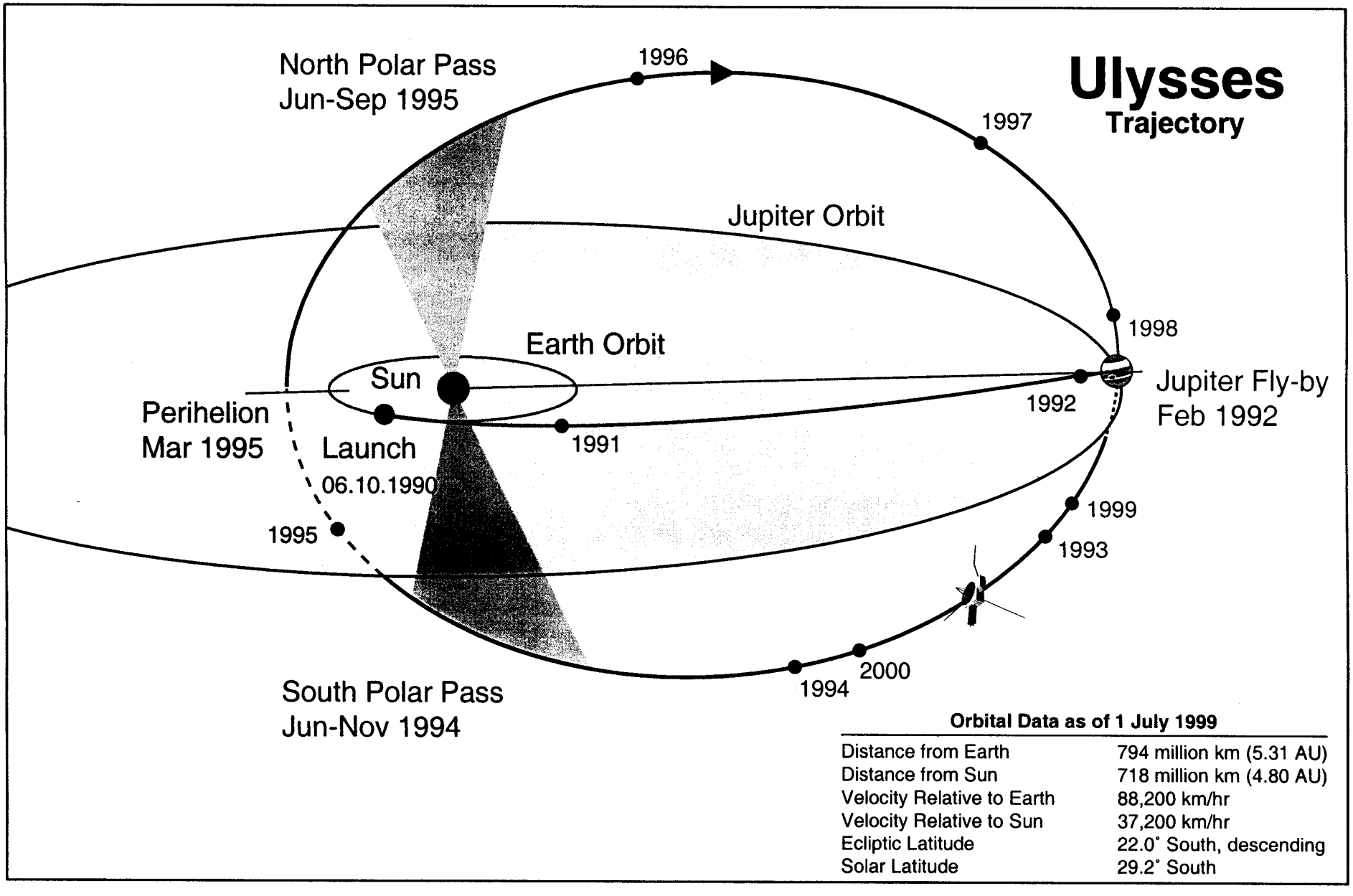

Orbital Data as of 1 July 1999

Distance from Earth	794 million km (5.31 AU)
Distance from Sun	718 million km (4.80 AU)
Velocity Relative to Earth	88,200 km/hr
Velocity Relative to Sun	37,200 km/hr
Ecliptic Latitude	22.0° South, descending
Solar Latitude	29.2° South

Rotational Discontinuity

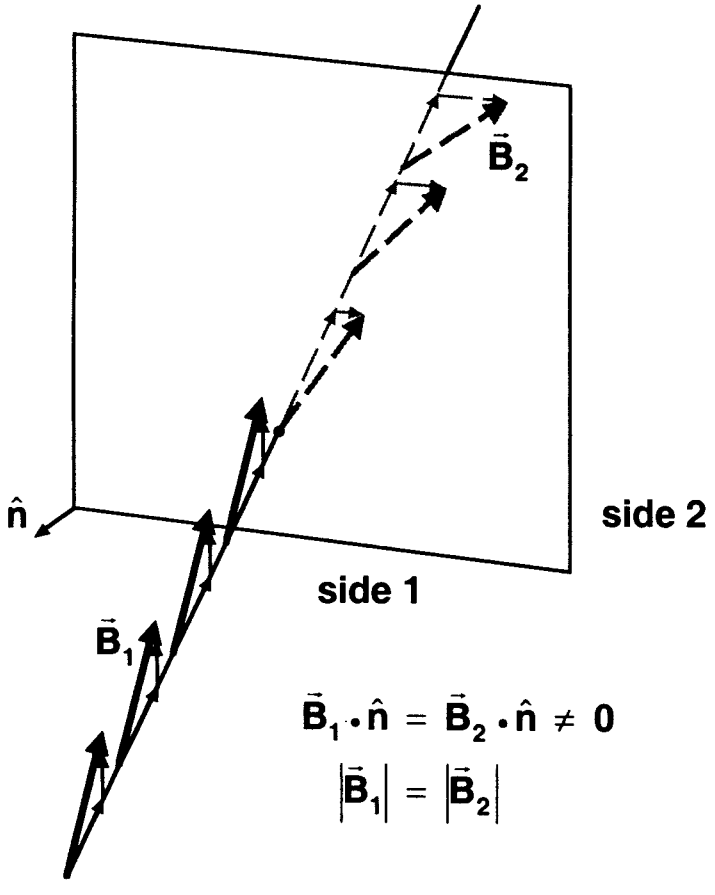

$$\vec{B}_1 \cdot \hat{n} = \vec{B}_2 \cdot \hat{n} \neq 0$$

$$|\vec{B}_1| = |\vec{B}_2|$$

Tangential Discontinuity

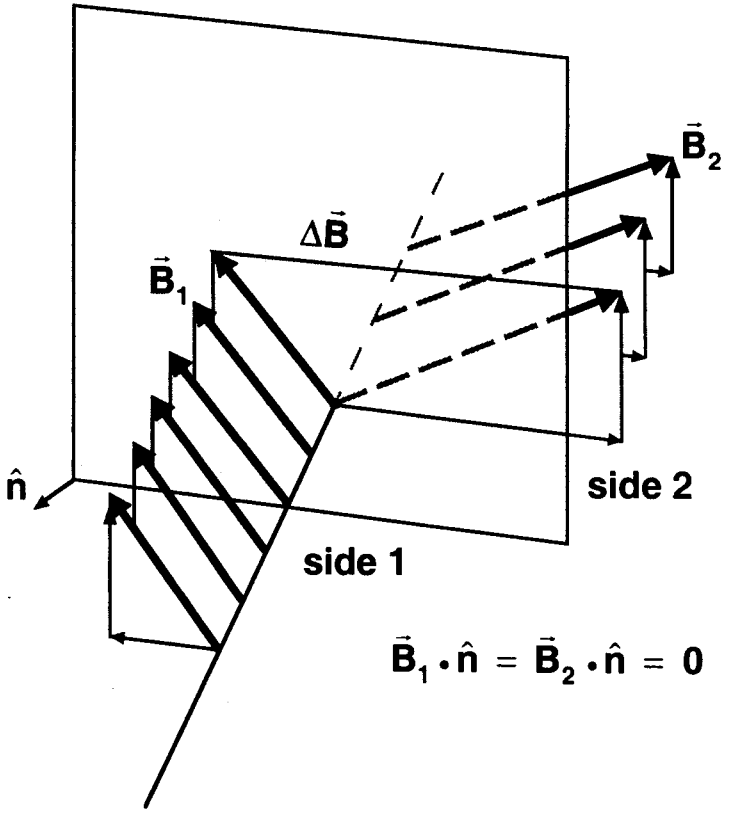

$$\vec{B}_1 \cdot \hat{n} = \vec{B}_2 \cdot \hat{n} = 0$$

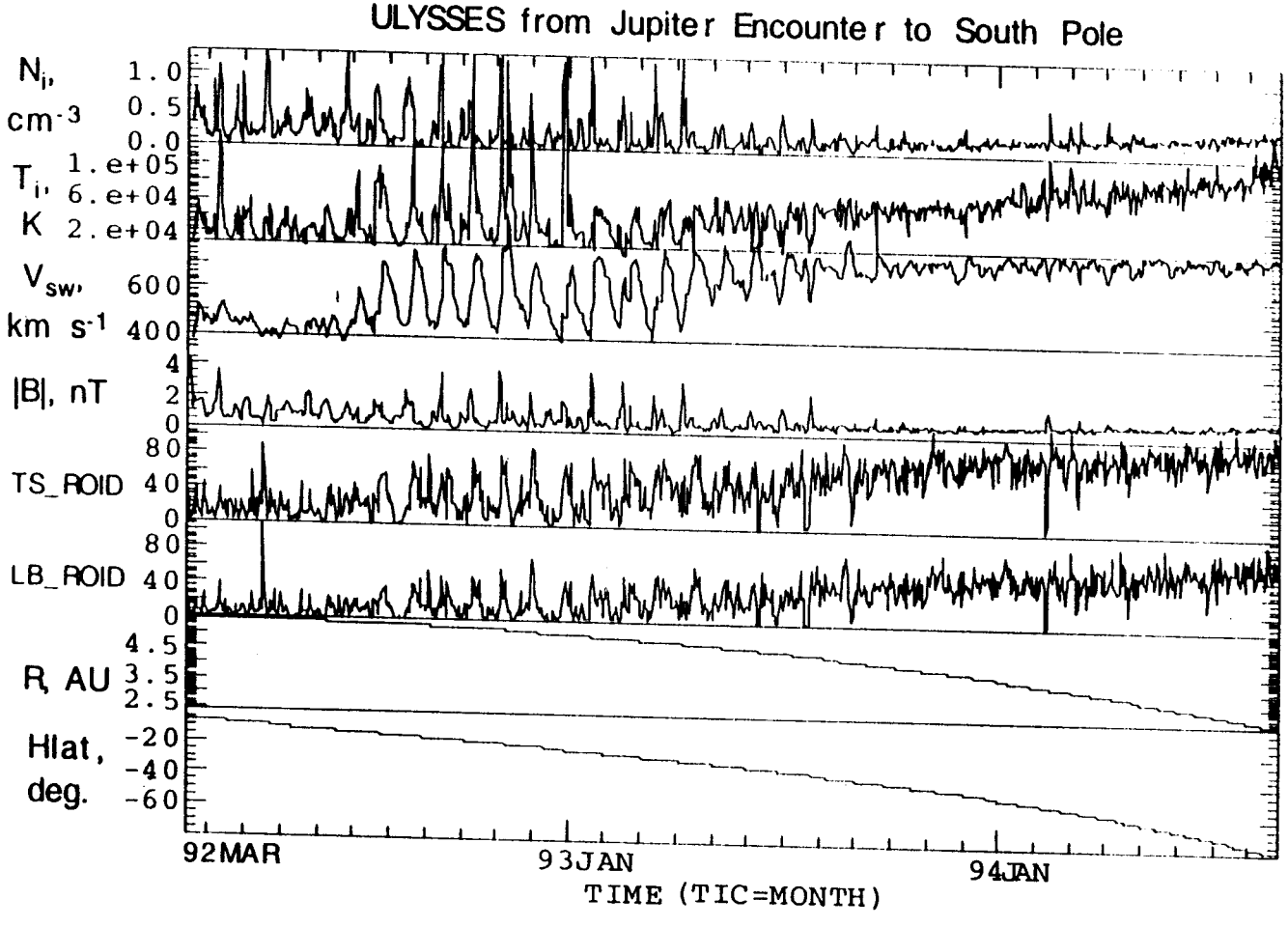
ULYSSES from Jupiter Encounter to South Pole
N_i, cm^{-3}
1.0
0.5
0.0
T_i, K
1.e+05
6.e+04
2.e+04
V_{sw}, km s^{-1}
600
400
|B|, nT
4
2
0
TS_ROID
80
40
0
LB_ROID
80
40
0
R, AU
4.5
3.5
2.5
Hlat, deg.
-20
-40
-60
92MAR
93JAN
94JAN
TIME (TIC=MONTH)

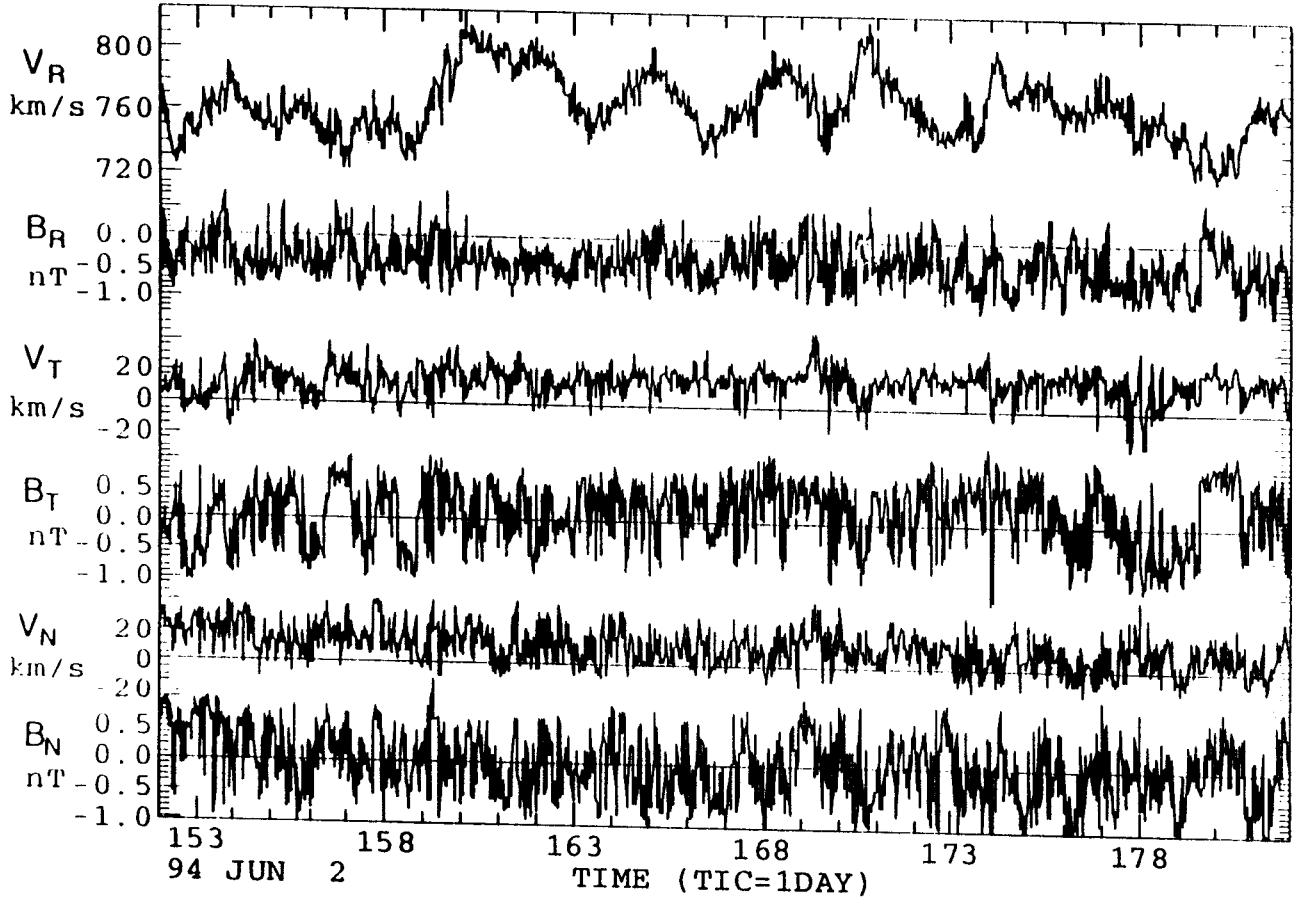
V_R
km/s
800
760
720
B_R
nT
0.0
-0.5
-1.0
V_T
km/s
20
0
-20
B_T
nT
0.5
0.0
-0.5
-1.0
V_N
km/s
20
0
-20
B_N
nT
0.5
0.0
-0.5
-1.0
153
158
163
168
173
178
94 JUN 2
TIME (TIC=1DAY)

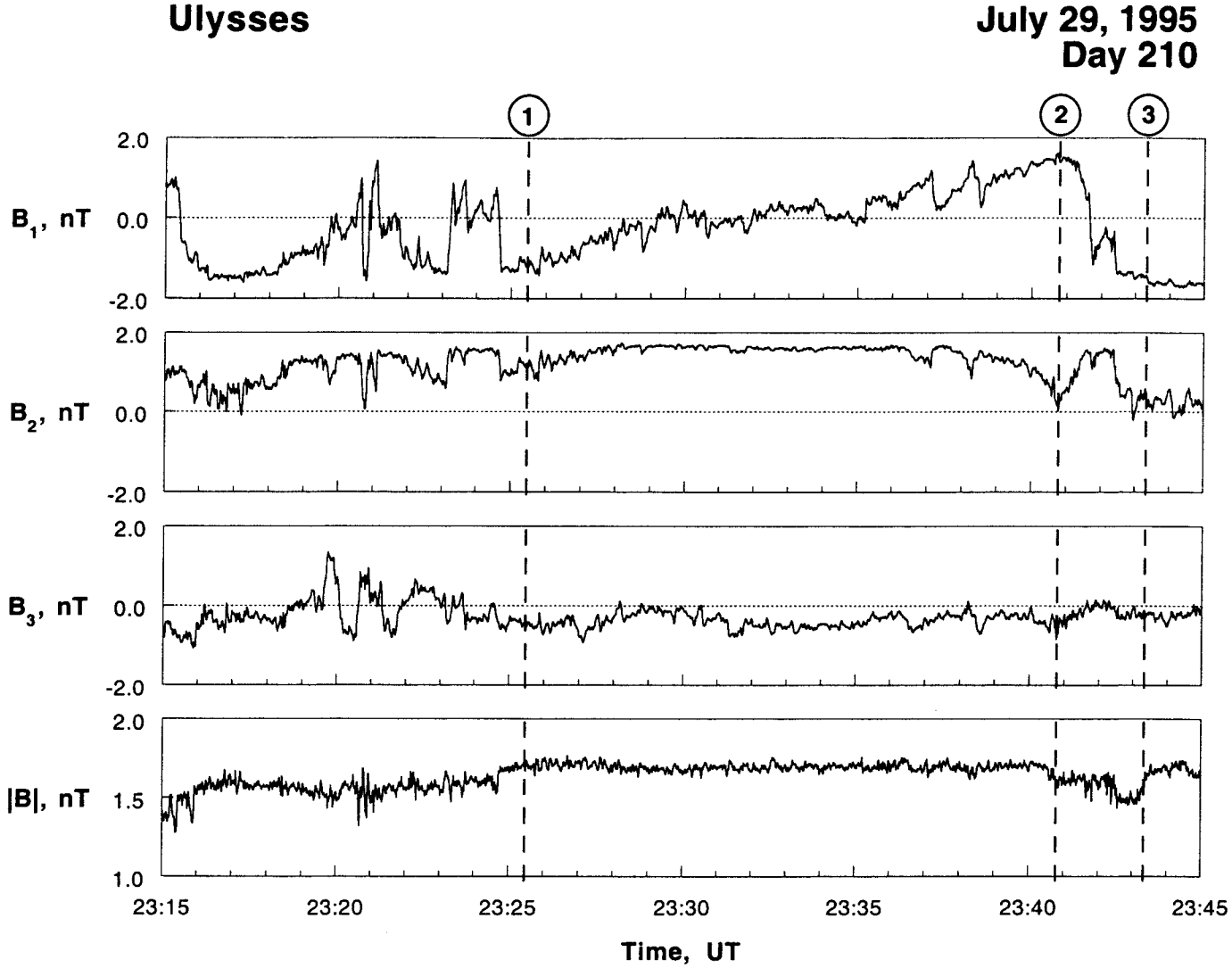
Ulysses
July 29, 1995
Day 210
1
2
3
B1, nT
B2, nT
B3, nT
|B|, nT
2.0
0.0
-2.0
1.5
1.0
23:15
23:20
23:25
23:30
23:35
23:40
23:45
Time, UT

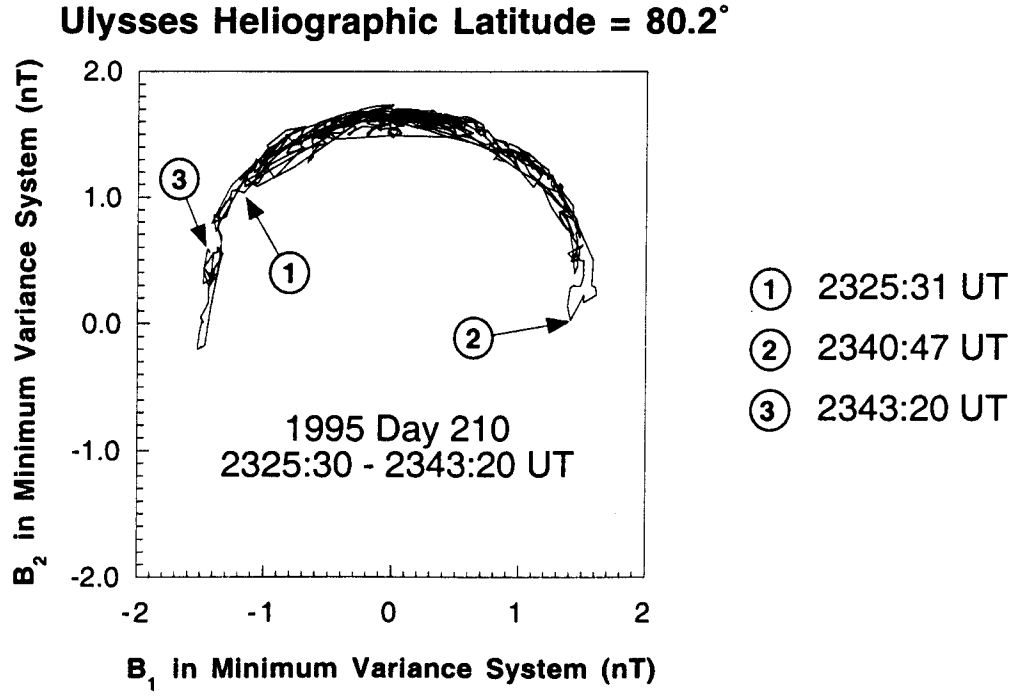
Ulysses Heliographic Latitude = 80.2°
B2 in Minimum Variance System (nT)
B1 in Minimum Variance System (nT)
2.0
1.0
0.0
-1.0
-2.0
-2
-1
0
1
2
1995 Day 210
2325:30 - 2343:20 UT
1 2325:31 UT
2 2340:47 UT
3 2343:20 UT

Spherical Waves

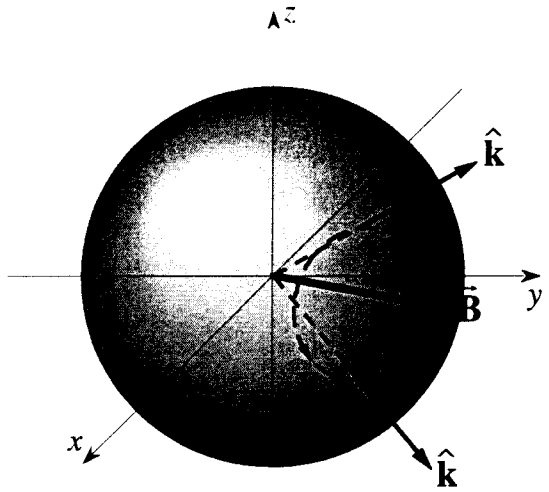

Circular Polarization

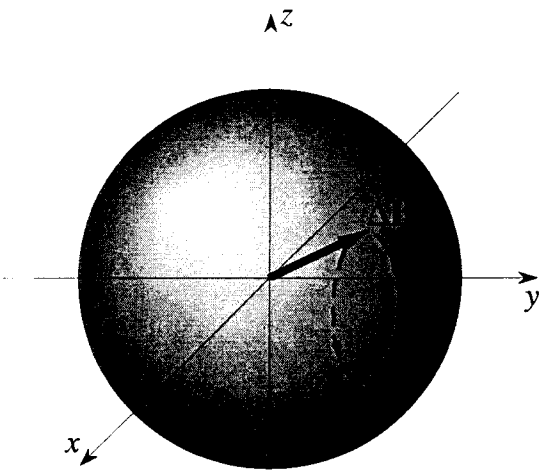

Elliptical Polarization

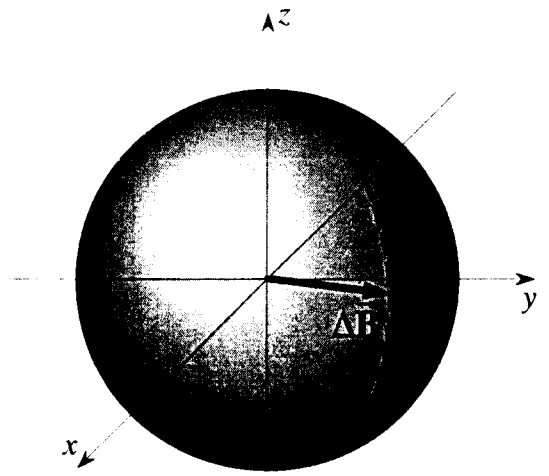

Arc Polarization

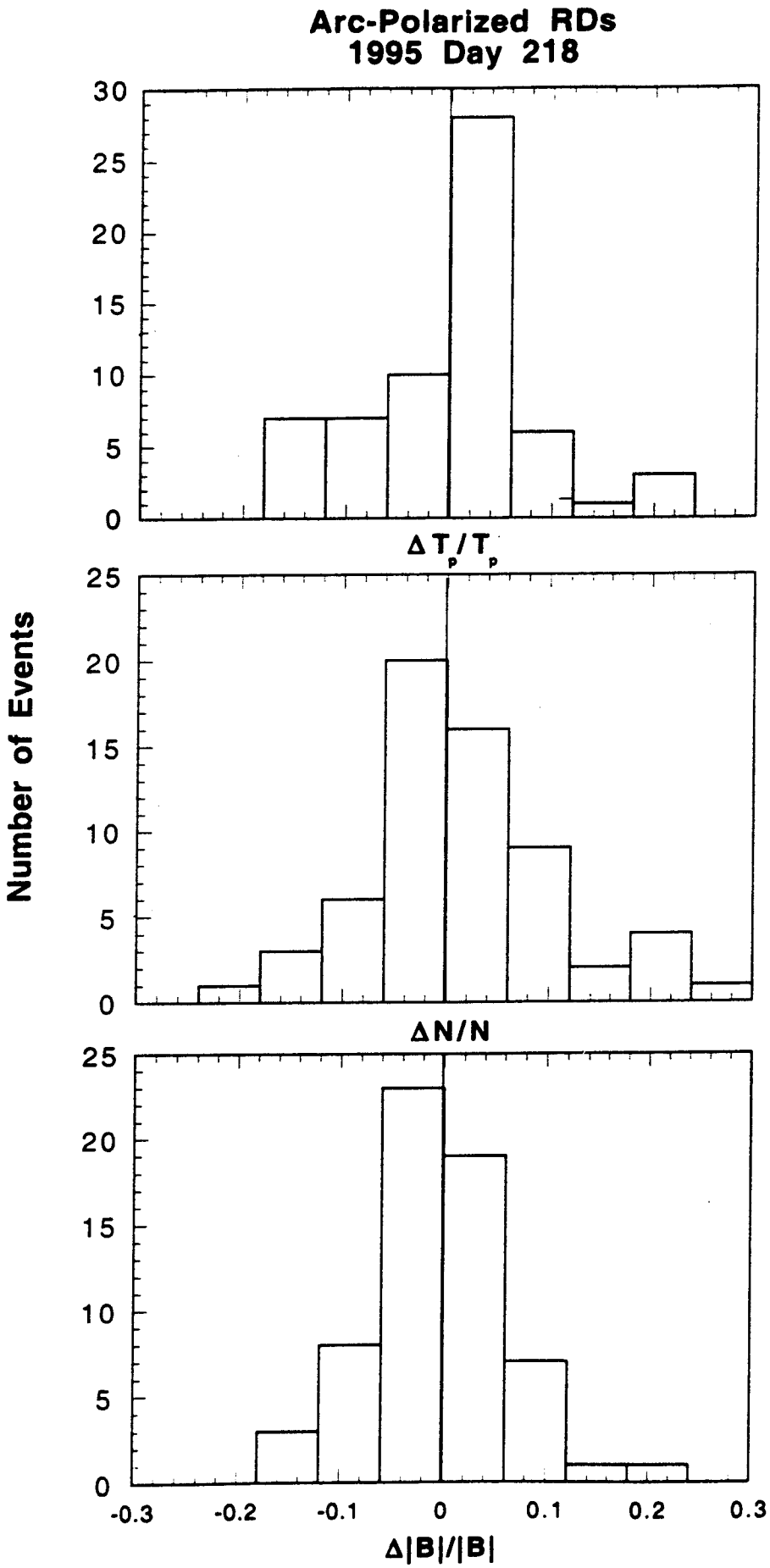
Arc-Polarized RDs
1995 Day 218
Number of Events
30
25
20
15
10
5
0
ΔT_p/T_p
25
20
15
10
5
0
ΔN/N
25
20
15
10
5
0
-0.3
-0.2
-0.1
0
0.1
0.2
0.3
Δ|B|/|B|

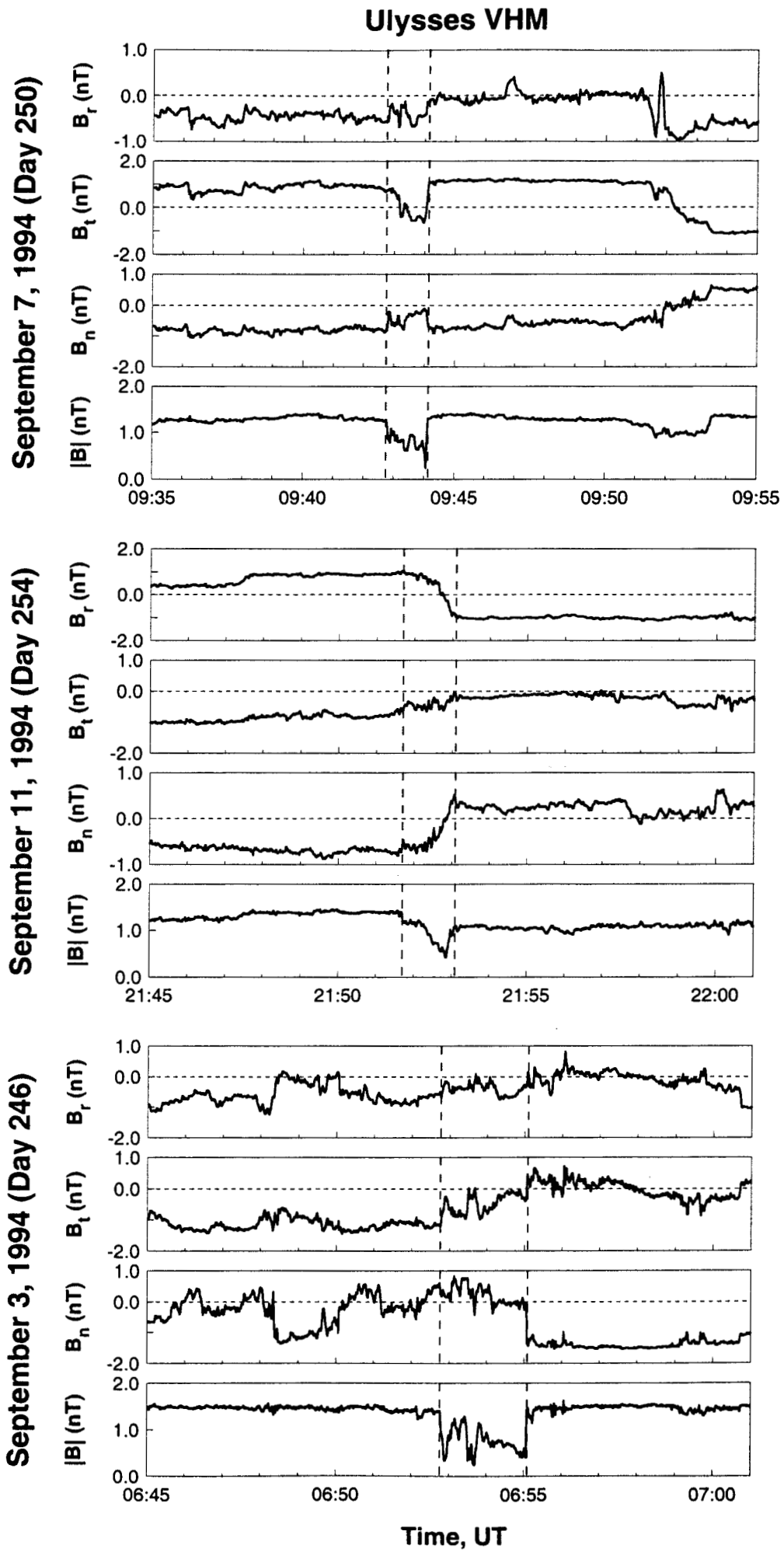
Ulysses VHM
September 7, 1994 (Day 250)
September 11, 1994 (Day 254)
September 3, 1994 (Day 246)
B_r (nT)
B_t (nT)
B_n (nT)
|B| (nT)
09:35
09:40
09:45
09:50
09:55
21:45
21:50
21:55
22:00
06:45
06:50
06:55
07:00
Time, UT

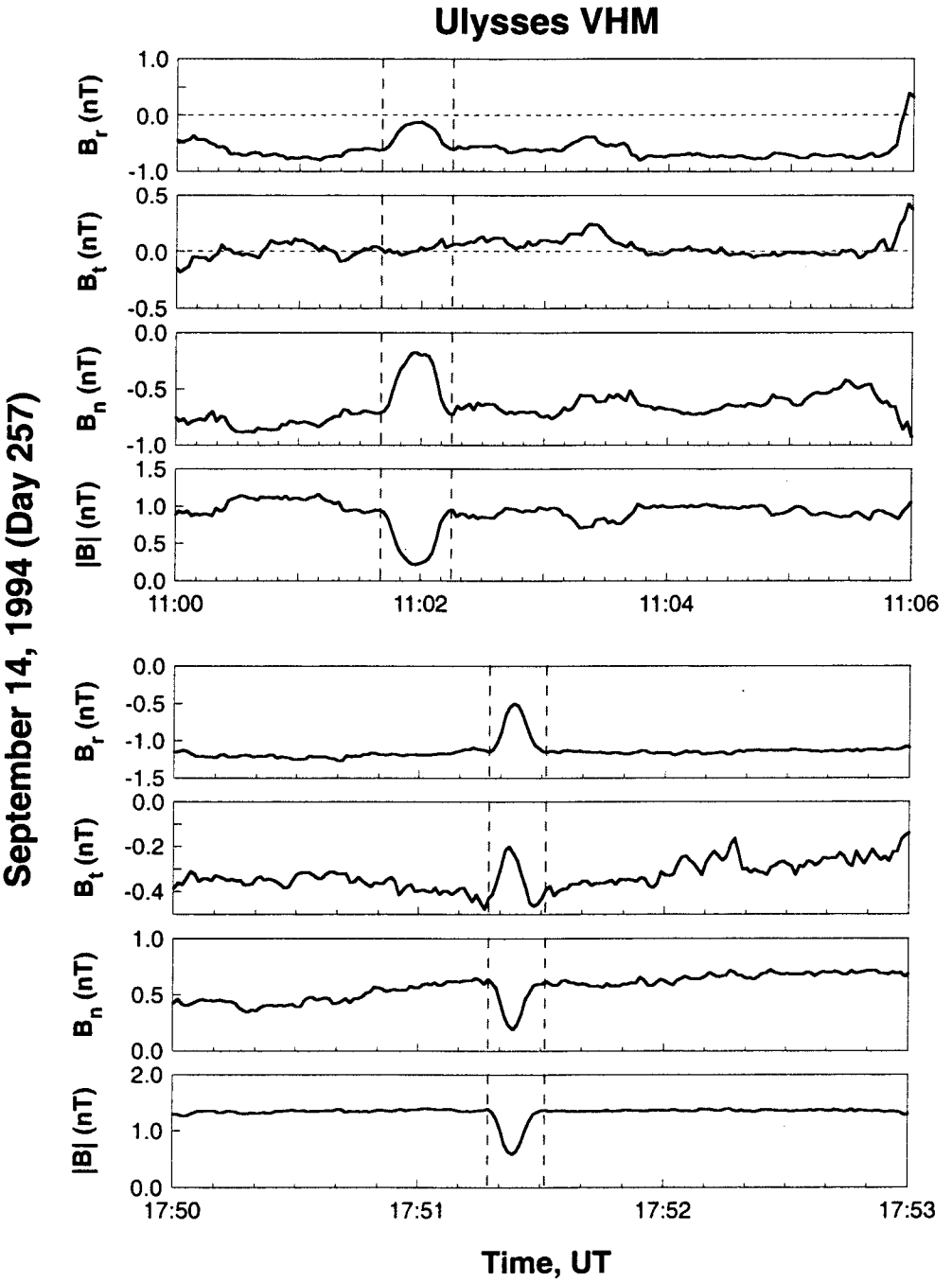
Ulysses VHM
September 14, 1994 (Day 257)
B_r (nT)
B_t (nT)
B_n (nT)
|B| (nT)
1.0
0.0
-1.0
0.5
0.0
-0.5
0.0
-0.5
-1.0
1.5
1.0
0.5
0.0
11:00
11:02
11:04
11:06
0.0
-0.5
-1.0
-1.5
0.0
-0.2
-0.4
1.0
0.5
0.0
2.0
1.0
0.0
17:50
17:51
17:52
17:53
Time, UT

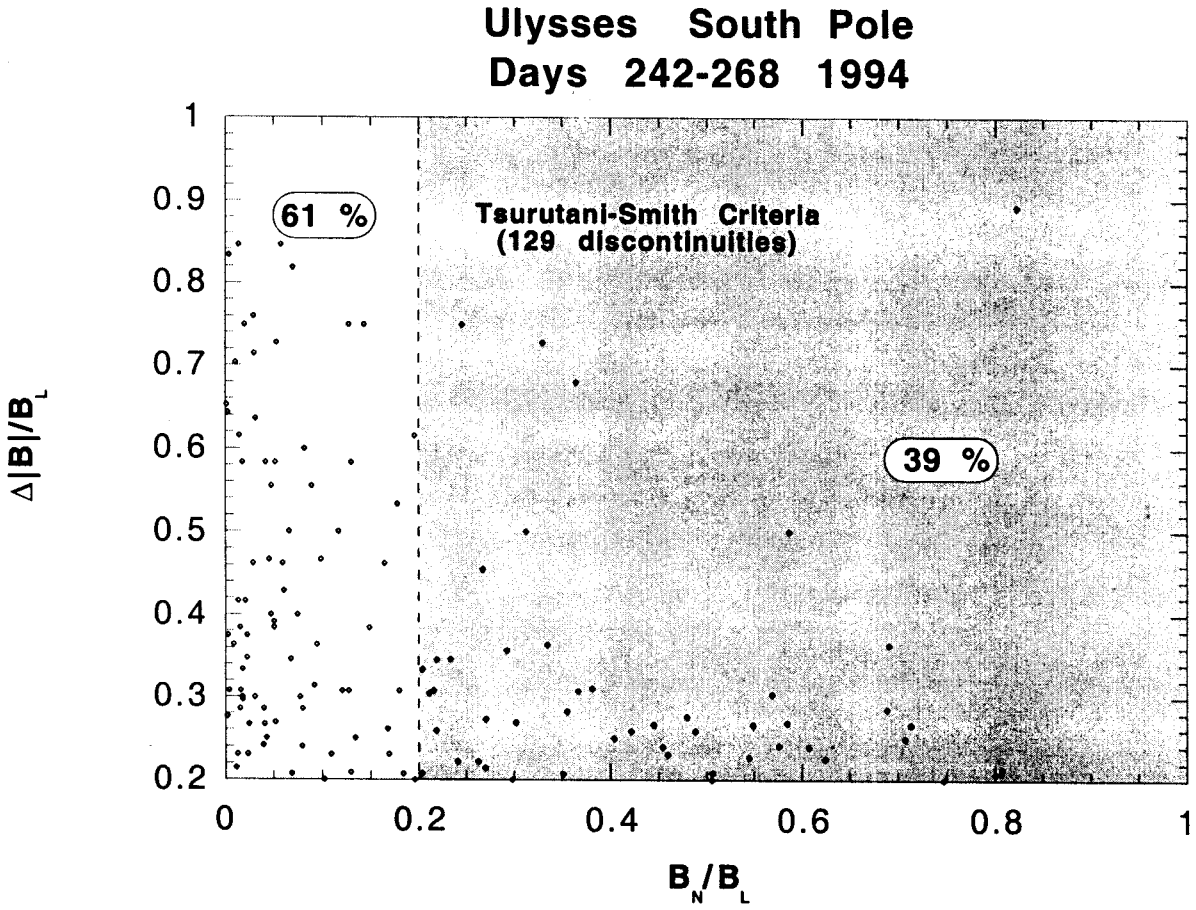
Ulysses South Pole
Days 242-268 1994
Tsurutani-Smith Criteria
(129 discontinuities)
61 %
39 %
Δ|B|/B_L
B_N/B_L
0
0.2
0.4
0.6
0.8
1
0.9
0.7
0.5
0.3

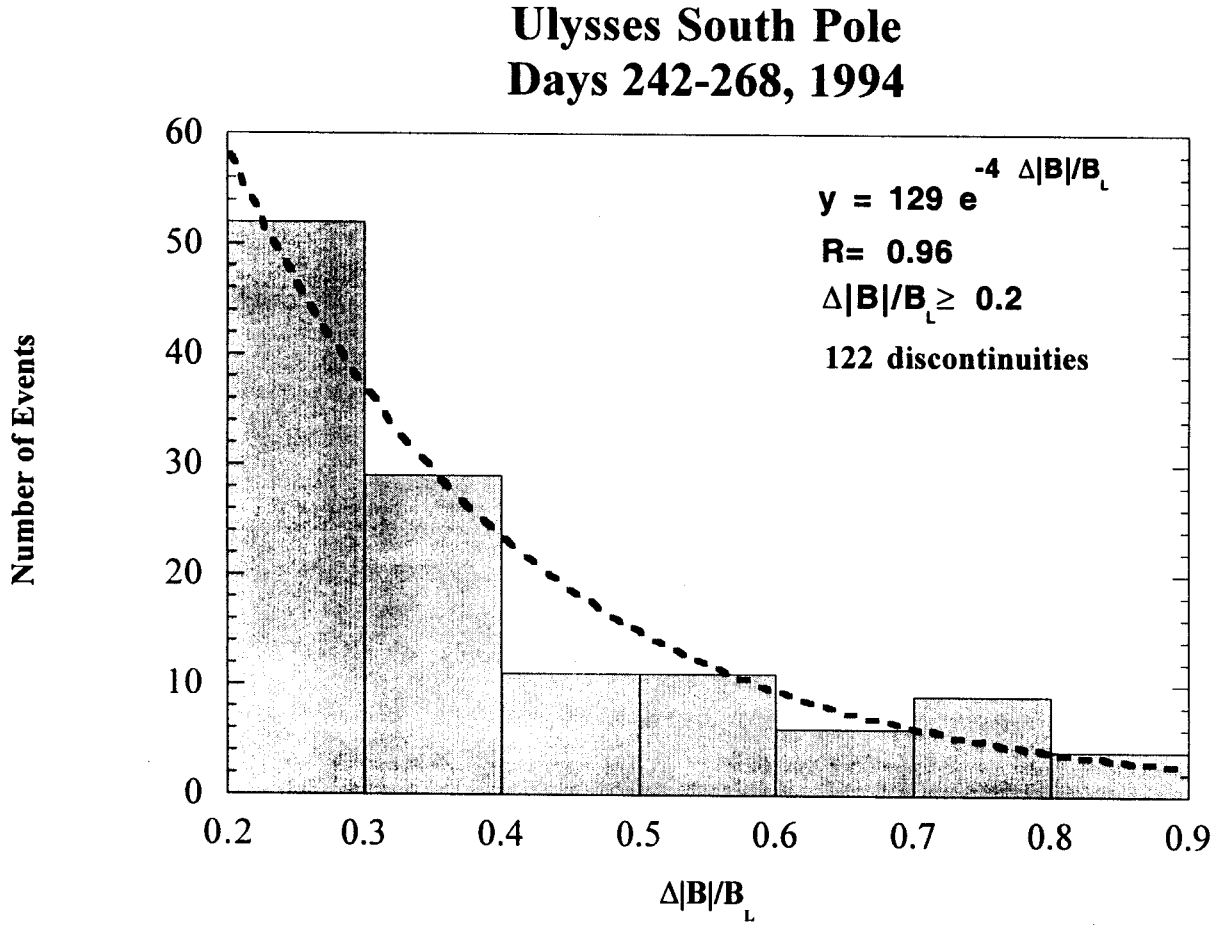
Ulysses South Pole
Days 242-268, 1994
Number of Events
60
50
40
30
20
10
0
0.2
0.3
0.4
0.5
0.6
0.7
0.8
0.9
Δ|B|/B_L
y = 129 e^-4 Δ|B|/B_L
R= 0.96
Δ|B|/B_L≥ 0.2
122 discontinuities

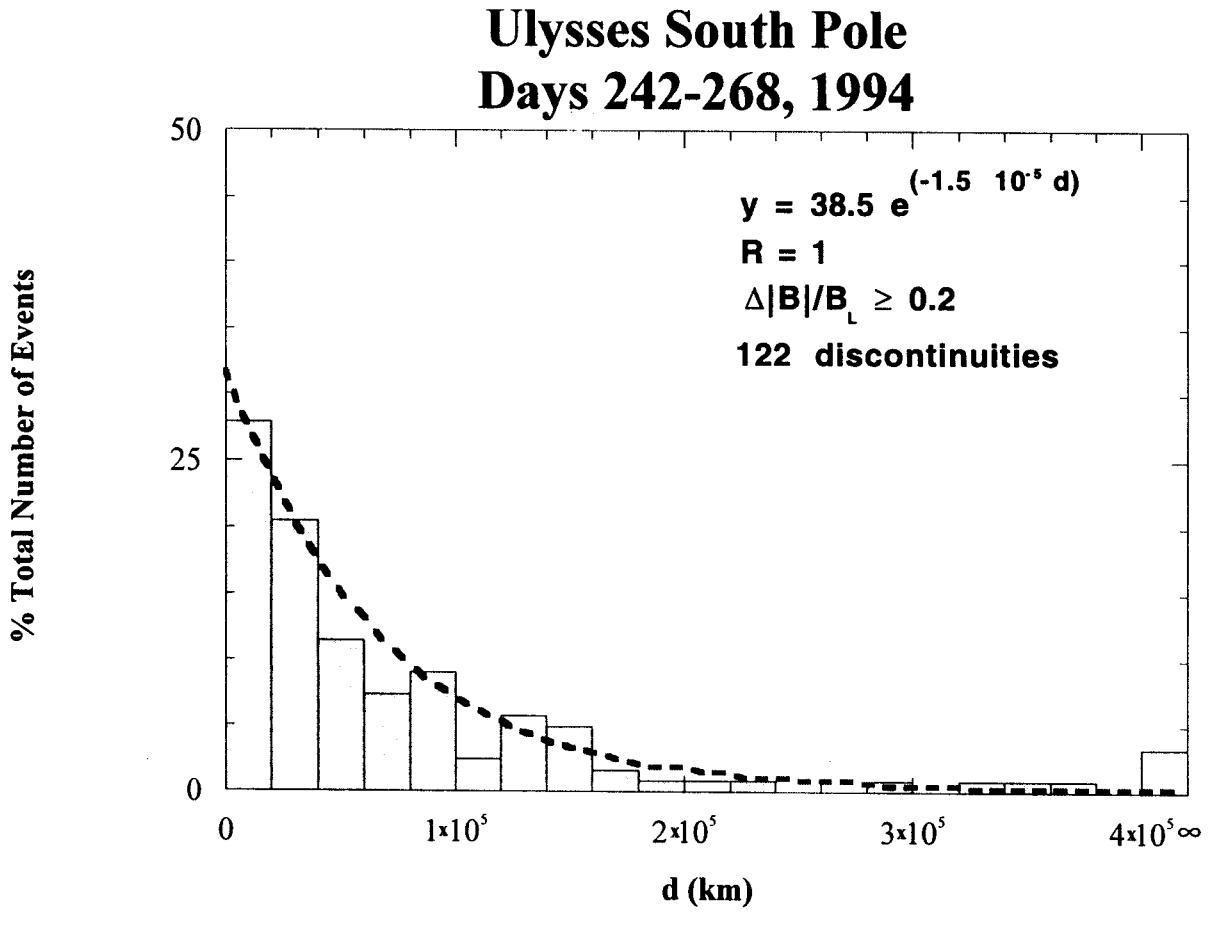
Ulysses South Pole
Days 242-268, 1994
y = 38.5 e^(-1.5 10^-5 d)
R = 1
Δ|B|/B_L ≥ 0.2
122 discontinuities
% Total Number of Events
50
25
0
0
1x10^5
2x10^5
3x10^5
4x10^5∞
d (km)

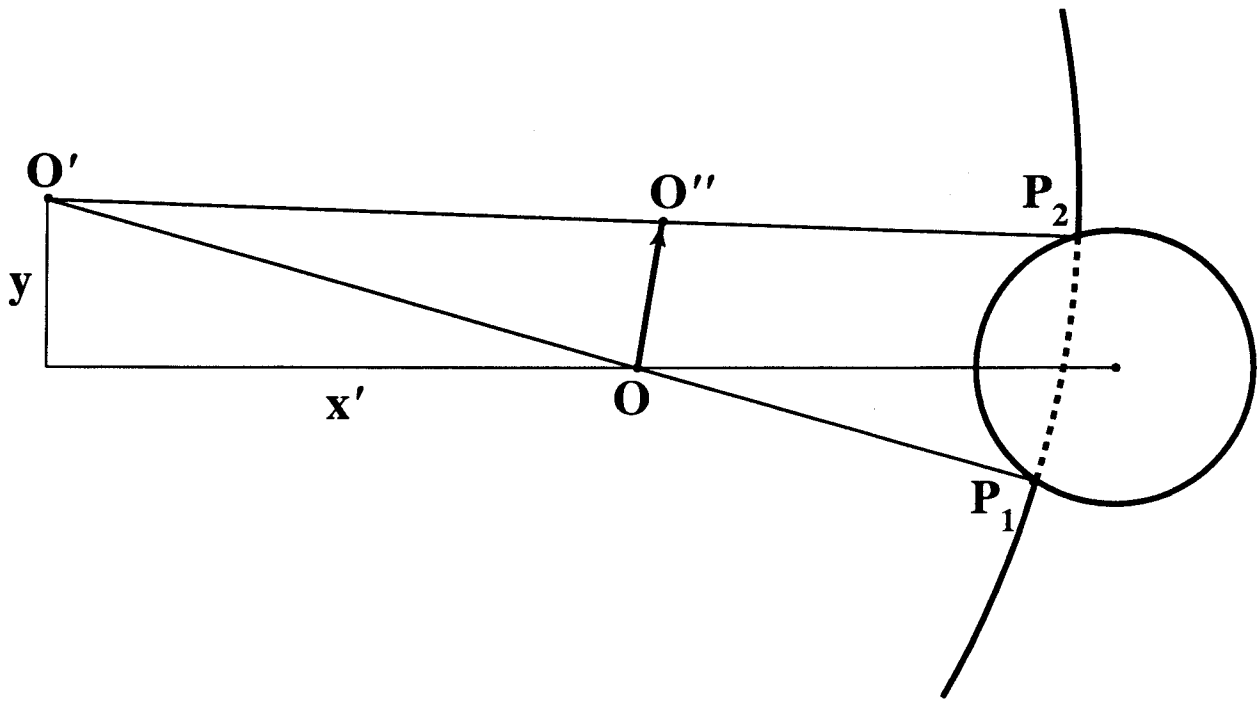
O′
O″
P2
y
x′
O
P1

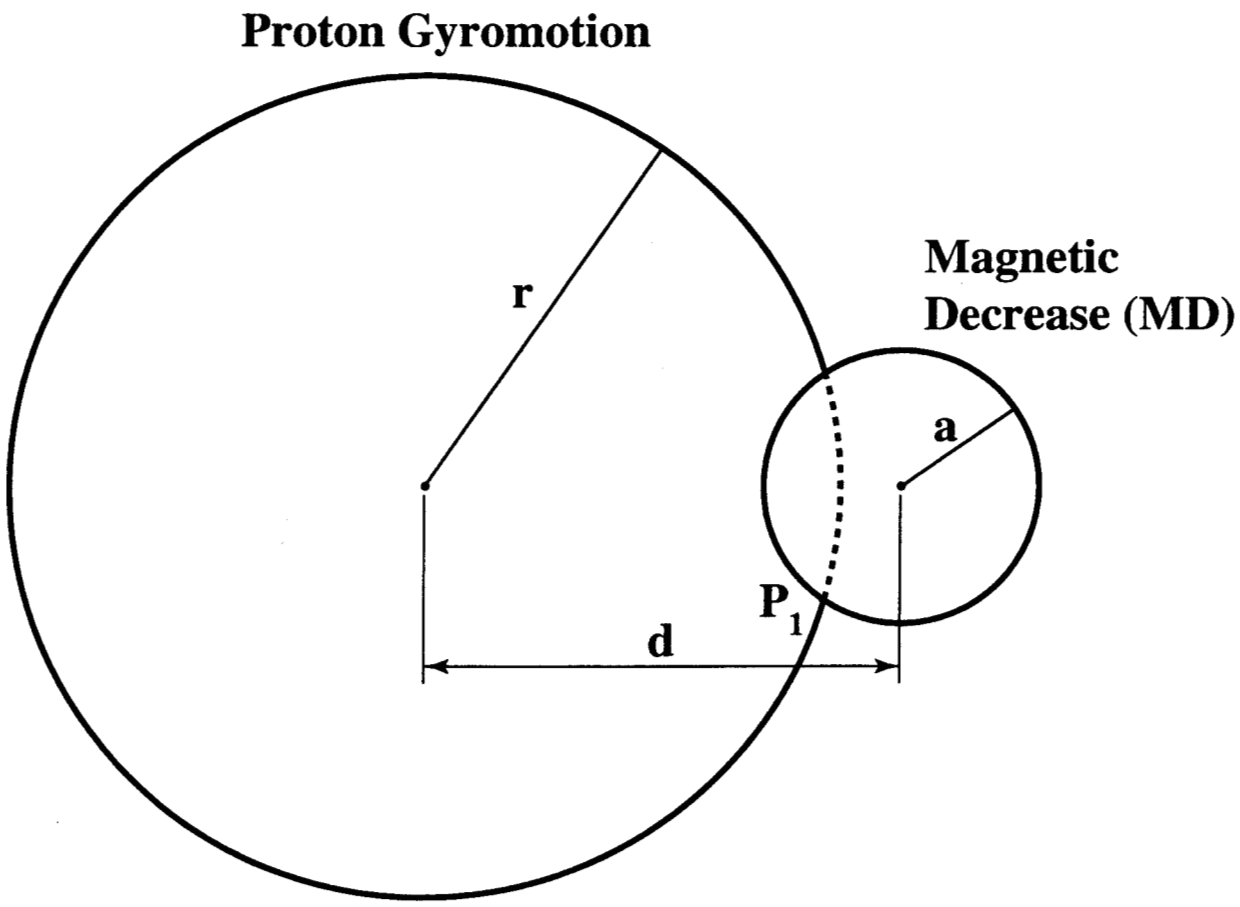
Proton Gyromotion
r
Magnetic
Decrease (MD)
a
P1
d